Applied Catalysis A, General 624 (2021) 118331

Contents lists available at ScienceDirect

Applied Catalysis A, General

journal homepage: www.elsevier.com/locate/apcata

Controlling the performance of a silver co-catalyst by a palladium core in TiO_2-photocatalyzed alkyne semihydrogenation and H_2 production

Shota Imai [a], Yasumi Kojima [a], Eri Fudo [a], Atsuhiro Tanaka [b,c], Hiroshi Kominami [b,*]

[a] Molecular and Material Engineering, Graduate School of Science and Engineering, Kindai University, 3-4-1, Kowakae, Higashiosaka, Osaka, 577-8502, Japan
[b] Department of Applied Chemistry, Faculty of Science and Engineering, Kindai University, 3-4-1 Kowakae, Higashiosaka, Osaka, 577-8502, Japan
[c] Precursory Research for Embryonic Science and Technology (PRESTO), Japan Science and Technology Agency (JST), Honcho, Kawaguchi, 332-0012, Japan

ARTICLE INFO

Keywords:
TiO_2
Photocatalyst
Co-catalyst
Core-shell
Semihydrogenation

ABSTRACT

Titanium (IV) oxide (TiO_2) having palladium (Pd) core-silver (Ag) shell nanoparticles (Pd@Ag/TiO_2) was prepared by using a two-step (Pd first and then Ag) photodeposition method. The core-shell structure of the nanoparticles having various Ag contents (shell thicknesses) and the electron states of Pd and Ag were investigated by transmission electron microscopy and X-ray photoelectron spectroscopy, respectively. The effect of the Pd core and the Ag shell was evaluated by hydrogenation of 4-octyne in alcohol suspensions of a photocatalyst under argon and light irradiation. 4-Octyne was fully hydrogenated to 4-octane over Pd/TiO_2, whereas 4-octyne was selectively hydrogenated to *cis*-4-octene over Pd(0.2)@Ag(0.5)/TiO_2. Further increase in the Ag content resulted in a decrease in the conversion of 4-octyne. Pd-free Ag/TiO_2 was inactive for hydrogenation of alkyne and induced coupling of active hydrogen species (H_2 production). Photocatalytic reactions at various temperatures revealed that the change in selectivity (semihydrogenation or H_2 production) can be explained by the difference in values of activation energy of the two reactions. An applicability test showed that the Pd@Ag/TiO_2 photocatalyst can be used for hydrogenation of various alkynes to alkenes.

1. Introduction

Metal nanoparticles have often been used as co-catalysts for semiconductor photocatalysts when the position of the conduction band bottom (CBB) is close to the reduction potential (RP) of target compounds [1–3]. The most popular co-catalyst is platinum (Pt), which has been used for hydrogen (H_2) production through proton (H^+) reduction (RP: 0 V vs NHE) with photogenerated electrons over titanium(IV) oxide (TiO_2) with an anatase structure (CBB: ca -0.3 V vs NHE) [4–9]. Metal nanoparticles are also utilized as co-catalysts for photocatalytic conversion of organic compounds. Palladium (Pd) exhibits excellent performance as a co-catalyst for dechlorination of chlorinated compounds [10] and hydrogenation of unsaturated C—C bonds [11] over a TiO_2 photocatalyst. Silver (Ag) [12], copper (Cu) [13] and rhodium (Rh) [14] also show specific and selective performance for photocatalytic reductive conversion of organic compounds. These results of past studies indicate that the combination of TiO_2 and metal nanoparticles widens the possibility of photocatalytic conversion.

Reductive conversion over a TiO_2 photocatalyst with a co-catalyst can be roughly separated into two processes [11–14]: 1) formation of active hydrogen species over the co-catalyst through the reaction of photogenerated electrons in the conduction band of TiO_2 and H^+ in the liquid phase and 2) reaction of a target compound and active hydrogen species over the co-catalyst. In other words, photocatalytic reduction over TiO_2 is regarded as a combination of photoinduced electron production over TiO_2 and catalytic reduction (hydrogenation) over the co-catalyst. As a side reaction, H_2 evolution by coupling of H^+ occurs if process 2) is slow over the co-catalyst. This means that the property of the co-catalyst loaded on TiO_2 controls the performance (reactivity and selectivity) of the photocatalytic reduction.

There are several methods to enhance the catalytic performance of metal catalysts and the use of two metals (bimetallic system) is one of the effective methods [15–19]. A bimetallic system can be roughly classified into alloy type and core-shell type. In the former type, it is generally difficult to understand the function of each element because the mixing level greatly depends on the preparation method, and the distribution of two elements on the surface and in the bulk (depth direction) should be considered for discussion of the catalytic performance. On the other hand, due to the simpler distribution of two elements in the core-shell type, discussion of the catalytic performance

* Corresponding author.
E-mail addresses: hiro@apch.kindai.ac.jp, kominami@kindai.ac.jp (H. Kominami).

https://doi.org/10.1016/j.apcata.2021.118331
Received 26 May 2021; Received in revised form 30 July 2021; Accepted 17 August 2021
Available online 19 August 2021

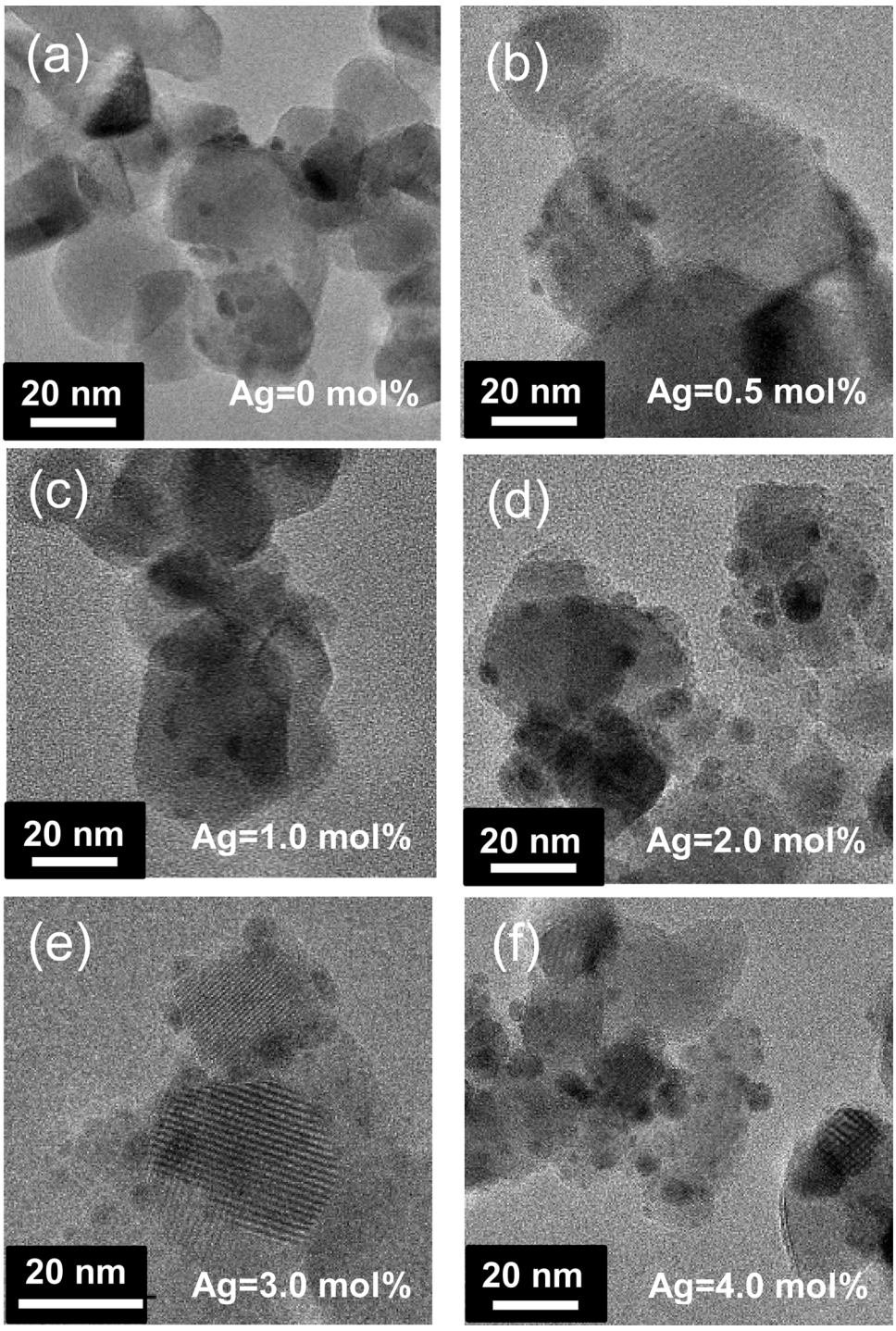

Fig. 1. TEM images of (a) Pd(0.2)/TiO_2, (b) Pd(0.2)@Ag(0.5)/TiO_2, (c) Pd(0.2)@Ag(1.0)/TiO_2, (d) Pd(0.2)@Ag(2.0)/TiO_2, (e) Pd(0.2)@Ag(3.0)/TiO_2 and (f) Pd(0.2)@Ag(4.0)/TiO_2.

of the bimetallic system would be easier than that of the alloy type. In our previous study, we achieved H_2-free semihydrogenation of alkyne over a Cu-loaded TiO_2 photocatalyst [13]. This photocatalyst converts alkynes to *cis*-alkenes selectively with complete suppression of isomerization and overhydrogenation of *cis*-alkenes, and the reaction rate greatly increased at a slightly elevated temperature with maintenance of a high level of *cis*-selectivity [20]. In photocatalytic semihydrogenation of alkynes, catalytic performance of Cu metal was greatly enhanced by introduction of a Pd core [21]. Inspired by the results obtained by using the Pd core-Cu shell, we were interested in another shell metal as the co-catalyst for semihydrogenation of alkynes. Silver metal exhibited negligible activity as a co-catalyst for photocatalytic alkyne hydrogenation [13]. In the field of catalytic (not photocatalytic) semihydrogenation under H_2, Pd core-Ag shell nanoparticles (Pd@Ag) supported on hydroxy apatite hydrogenated alkynes to alkenes in high yields [15]. The authors of the paper reported that 1) H_2 was supplied to the Ag shell from the Pd core, 2) the Ag shell worked as active sites for semihydrogenation, and 3) Ag played a role to inhibit overhydrogenation of alkenes over Pd. Since the mechanisms of catalytic hydrogenation in the presence of H_2 and photocatalytic hydrogenation

Table 1
Average diameter of co-catalysts, standard deviation and thickness of the Ag shell calculated by TEM observation.

Photocatalyst	D_{ave} / nm	σ / nm	Thickness of Ag shell[a] / nm
Pd(0.2)/TiO_2	2.5	0.6	–
Pd(0.2)@Ag(0.5)/TiO_2	3.6	0.7	0.6
Pd(0.2)@Ag(1.0)/TiO_2	4.7	1.0	1.1
Pd(0.2)@Ag(2.0)/TiO_2	5.7	1.7	1.6
Pd(0.2)@Ag(3.0)/TiO_2	6.5	1.6	2.0
Pd(0.2)@Ag(4.0)/TiO_2	7.5	1.9	2.5

[a] The values of thickness of Ag shell were calculated from following equation. Thickness of Ag shell $= \frac{D_{ave}(Pd(0.2)@Ag(X)/TiO_2) - D_{ave}(Pd(0.2)/TiO_2)}{2}$.

in the absence of H_2 are different, investigation of photocatalytic hydrogenation over TiO_2 having Pd@Ag (Pd@Ag/TiO_2) and discussion of the functions of Pd and Ag in alkyne hydrogenation are valuable for designing photocatalysts having core-shell particles.

We prepared Pd@Ag/TiO_2 by a two-step photodeposition method [22,23] and used it for photocatalytic hydrogenation of alkyne in an alcohol suspension without the use of H_2 gas. We report here 1) characterization of Pd@Ag/TiO_2 having various Ag contents, 2) evaluation of photocatalytic alkyne hydrogenation over Pd@Ag/TiO_2 and 3) discussion of the functions of Pd and Ag in the alkyne hydrogenation based on the kinetics of Pd@Ag/TiO_2.

2. Experimental

2.1. Preparation of Ag/TiO_2 and Pd/TiO_2

Palladium(II) chloride ($PdCl_2$) and silver(I) nitrate ($AgNO_3$) (FUJIFILM Wako Pure Chemical Co., Tokyo, Japan) were used as received without further purification. In 10 cm^3 of a 50 vol% aqueous 2-propanol solution containing $PdCl_2$ or $AgNO_3$ in a Pyrex test tube, TiO_2 (P 25 supplied by Nippon Aerosil, Tokyo, Japan) was suspended, and the gas phase (air) of the test tube was replaced with argon (Ar). After plugging the test tube with a rubber septum, the suspension under continuous stirring was photoirradiated using a high-pressure mercury lamp (Koike Precision Instruments, Hyogo, Japan) for 2 h in a water bath kept at 293 K. The resulting powder was washed repeatedly with distilled water and dried for 2 h *in vacuo*.

2.2. Preparation of Pd@Ag/TiO_2

For preparation of Pd@Ag/TiO_2, 0.2 mol%Pd/TiO_2 (Pd(0.2)/TiO_2) was used as the starting material. An Ag shell was introduced onto Pd particles with a photodeposition method that had been used as the method for preparation of Au@Cu/CeO_2 [22] and Au@Pd/TiO_2 [23]. The amount of Ag (X) was changed from 0 to 4.0 mol% and the samples are designated as Pd(0.2)@Ag(X)/TiO_2 hereafter.

2.3. Characterization

Transmission electron microscopy (TEM) and energy dispersive X-ray analysis (EDX) were used to observe nanoparticles loaded on TiO_2 over a JEM-3010 (JEOL, Tokyo, Japan) operated at 200 kV in the Joint Research Center (JRC) at Kindai University. X-ray photoelectron spectroscopy (XPS) spectra of Ag/TiO_2 and Pd(0.2)@Ag(X)/TiO_2 were measured using an AXIS-NOVA ESCA (Shimadzu, Kyoto, Japan) in JRC at Kindai University.

2.4. Photocatalytic hydrogenation of 4-octyne at 293 K

Metal-loaded TiO_2 (50 mg) was suspended in 5 cm^3 of 2-propanol containing 4-octyne (*ca.* 60 μmol) in a test tube, which was sealed with a rubber septum and then photoirradiated under Ar at 293 K with the high-pressure mercury lamp. The amounts of 4-octyne, *cis*-4-octene, *trans*-4-octene and octane were determined with an FID-type gas chromatograph (GC-2025, Shimadzu) equipped with a DB-1 column. Toluene was used as an internal standard sample. The internal standard solution (0.1 cm^3) was added to the reaction solution (3 cm^3). After the mixture had been stirred for 5 min, the amounts of 4-octyne, *cis*-4-octene, *trans*-4-octene and octane were determined from the ratios of the peak areas to the peak area of toluene. The amount of H_2 as the reduction product of protons (H^+) and the amount of acetone as the oxidation product of 2-propanol were determined with a TCD-type gas chromatograph (GC-8A, Shimadzu) equipped with an MS-5A column and an FID-type gas chromatograph (GC-2025, Shimadzu) equipped with a DB-WAX column, respectively.

2.5. Action spectrum

A multi-wavelength irradiation monochromator (MM-3, Bunkoukeiki, Tokyo, Japan) was used to obtain apparent quantum efficiency (AQE), and light intensity was determined by using a spectroradiometer (USR-45D, Ushio, Tokyo, Japan). The amount of 4-octyne was determined in the same way as that for the photocatalytic reaction (Section 2.3). Using Eq. (1), AQE at each centered wavelength of light was calculated from the amount of *cis*-4-octene formed and the number of photons irradiated:

$$\mathrm{AQE} = \frac{2 \times \text{amount of } cis\text{-octene formed}}{\text{amount of incident photons}} \times 100 \quad (1)$$

2.6. Kinetics study (photocatalytic reaction at various temperatures)

A reaction mixture containing 2-propanol (5 cm^3), Pd(0.2)@Ag(0.5)/TiO_2 (50 mg) and 4-octyne (90 μmol) in a test tube, which was set in a water bath made of glass kept at various temperatures, was photoirradiated with a UV LED (PJ-1505-2CA, CCS Inc., Kyoto).

2.7. Catalytic hydrogenation of 4-octyne under H_2 in the dark

Metal-loaded TiO_2 (50 mg) was suspended in 5 cm^3 of 2-propanol containing 4-octyne (*ca.* 60 μmol) in a test tube. The test tube was sealed with a rubber septum under H_2 and the mixture was stirred in a water bath kept at 293 K in the dark. The amount of 4-octyne was determined in the same way as that for the photocatalytic reaction (Section 2.4).

3. Results and discussion

3.1. Characterization of Pd(0.2)@Ag(X)/TiO_2

Fig. 1(a) shows a TEM photograph of Pd(0.2)/TiO_2, indicating that Pd nanoparticles were successfully loaded on TiO_2. From the particle size distribution (Fig. S1(a)), the average diameter of the particles (D_{ave}) was determined to be 2.5 nm. Nanoparticles were also observed in TEM photographs of Pd(0.2)@Ag(X)/TiO_2 (Fig. 1(b)–(f)) and the values of D_{ave} were larger than that of Pd(0.2)/TiO_2 (Table 1), indicating that Ag was deposited on Pd nanoparticles. Table 1 also shows the thickness of

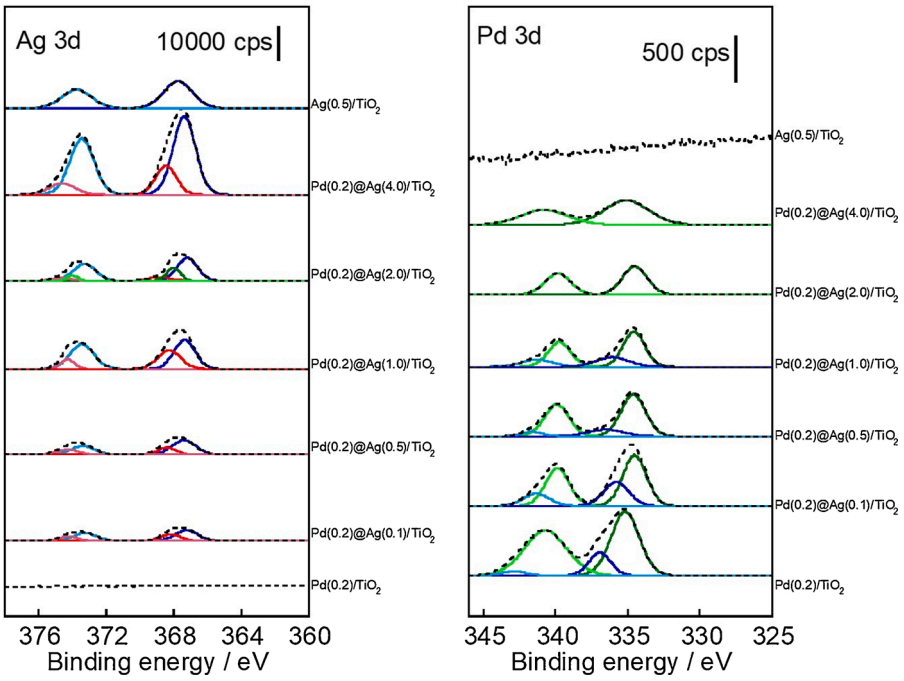

Fig. 2. XPS spectra of Pd(0.2)@Ag(X)/TiO_2 (X = 0, 0.1, 0.5, 1.0, 2.0, 4.0) and Ag(0.5)/TiO_2; left: Ag 3d, right: Pd 3d.

the Ag shell calculated from two values of D_{ave} of Pd(0.2)/TiO_2 and Pd(0.2)@Ag(X)/TiO_2. The thickness of the Ag shell gradually increased with an increase in the Ag content (X). In the TEM-EDX map of Pd(0.2)@Ag(0.5)/TiO_2 (Fig. S2), Ag was deposited on Pd particles and the noise levels of Ag and Pd on TiO_2 were same, indicating that Ag and Pd form the core-shell structure.

Fig. 2(a) shows Ag 3d XPS spectra of Ag(0.5)/TiO_2 and Pd(0.2)@Ag(X)/TiO_2. Peaks assignable to Ag^0 were observed in the spectrum of Ag(X)/TiO_2 at around 367.9 eV and 373.9 eV [24]. In the spectra of Pd(0.2)@Ag(X)/TiO_2, peaks assignable to Ag^0 and Ag^+ were observed and the intensity of the peaks increased with increase in X. We noted that the peaks of Pd(0.2)@Ag(X)/TiO_2 were slightly shifted to the lower binding energy, indicating that a part of Ag in the shell of these samples was in an electron-rich state. Fig. 2(b) shows Pd 3d XPS spectra of the same samples and peaks were observed at around 335.0 eV and 340.3 eV. The shape of Pd 3d spectra of Pd(0.2)@Ag(X)/TiO_2 was similar to that of Pd 3d spectra of Pd@Cu/TiO_2 [21] prepared by the same method, in which both Pd^0 and Pd^{2+} [25] were present. Peak intensity decreased with an increase in X, which is consistent with the increase in the thickness of the Ag shell. From the results of TEM and XPS analyses, it can be concluded that the electronic state of the Ag shell is affected by the Pd core, especially in the samples having a thinner Ag shell. Since Pd-Ag/TiO_2 samples were prepared by two step-photodeposition method (Pd first and then Ag) at room temperature, a high level of Pd and Ag alloying is ruled out and alloying of Pd and Ag may occur only at the interface of Pd particles and Ag deposited on Pd.

3.2. *Effects of introduction of an Ag shell on photocatalytic hydrogenation over Pd(0.2)@Ag(X)/TiO_2*

Table 2 shows 4-octyne conversion and product selectivity over Pd/TiO_2 and Pd(0.2)@Ag(X)/TiO_2 for 1 h. For comparison, the results for Pd-free Ag/TiO_2 are also shown in Table 2. Conversion (Conv.) and selectivity (Sel.) were calculated by Eqs. (2) and (3), respectively:

$$\text{Conv.} = \frac{n_0(\text{4-Octyne}) - n(\text{4-Octyne})}{n_0(\text{4-Octyne})} \times 100 \quad (2)$$

Table 2
Hydrogenation of 4-octyne over various photocatalysts.[a]

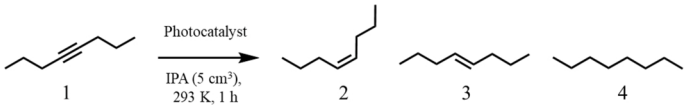

Entry	Photocatalyst	Conv. of 1[b] / %	Sel. of 2[b] / %	Sel. of 3[b] / %	Sel. of 4[b] / %
1	Ag(0.5)/TiO_2	0	0	0	0
2	Pd(0.2)/TiO_2	>99	0	0	98
3	Pd(0.2)@Ag(0.1)/TiO_2	>99	94	5	1
4	Pd(0.2)@Ag(0.5)/TiO_2	>99	99	1	0
5	Pd(0.2)@Ag(1.0)/TiO_2	71	98	0	0
6	Pd(0.2)@Ag(2.0)/TiO_2	38	>99	0	0
7	Pd(0.2)@Ag(3.0)/TiO_2	22	97	0	0
8	Pd(0.2)@Ag(4.0)/TiO_2	8	>99	0	0

[a] Reaction conditions: photocatalyst (50 mg), 4-octyne (*ca.* 60 μmol), 2-propanol (5 cm^3), 293 K and under Ar.
[b] Determined by GC using an internal standard.

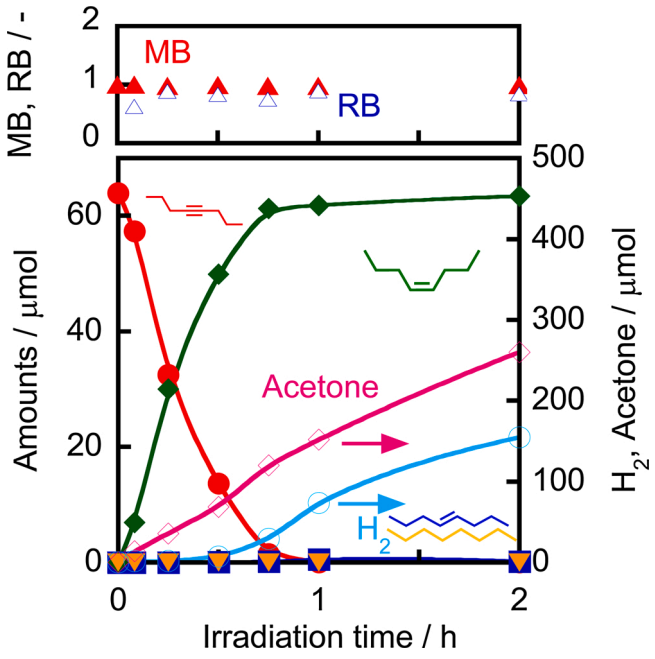

Fig. 3. Time courses of amounts of 4-octyne (●), *cis*-4-octene (◆), *trans*-4-octene (■), octane (▼), H_2 (○) and acetone (◇) formed and values of MB (▲) and RB (△) in 2-propanol suspensions of Pd(0.2)@Ag(0.5)/TiO_2 under a deaerated condition at 293 K.

$$\text{Sel.} = \frac{\text{n(product)}}{\text{n}_0\text{(4-Octyne)} - \text{n(4-Octyne)}} \times 100 \quad (3)$$

No 4-octyne was converted over Ag/TiO_2 (Entry 1), indicating Ag/TiO_2 was inactive for photocatalytic hydrogenation of alkyne under this condition. On the other hand, 4-octyne was fully hydrogenated to octane when Pd/TiO_2 was used (Entry 2), indicating that Pd/TiO_2 has strong hydrogenation activity. When Pd/TiO_2 was modified with 0.1 mol%Ag, production of octane was greatly suppressed and *cis*-4-octene was obtained with a high selectivity (94 %) together with a small amount of *trans*-4-octene (Entry 3). Results of Entries 2 and 3 show that Pd metals are not the active sites for semihydrogenation. The selectivity of *cis*-4-octene further increased to 99 % when 0.5 mol%Ag was introduced to Pd/TiO_2 (Entry 4). Almost stoichiometric conversion of 4-octyne to *cis*-4-octene (99 %), *i.e.*, 99 % selectivity at >99 % conversion, was contrast with general results (a high alkene selectivity at a low alkyne conversion). More introduction of Ag resulted in a decrease in the conversion of 4-octyne with maintenance of high selectivity to *cis*-4-octene (Entries 5-8). These results indicate that excessive activity of Pd nanoparticles is suppressed and changed to mild and selective by the introduction of a thin Ag shell. Almost ideal performance was achieved when X was 0.5 and the catalytic performance gradually became closer to that of Ag/TiO_2 with an increase in the thickness of the Ag shell. Changes in the catalytic performance were in an agreement with the electronic state of Ag, *i.e.*, Ag in an electron-rich state is important as the active sites for selective hydrogenation of 4-octyne to *cis*-4-octene. These results show that inert Ag co-catalyst was activated by a Pd core.

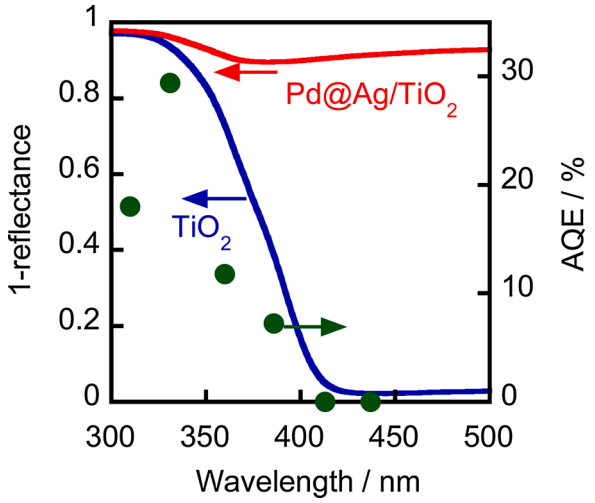

Fig. 4. Absorption spectra of TiO_2 and Pd(0.2)@Ag(0.5)/TiO_2 and action spectrum of Pd(0.2)@Ag(0.5)/TiO_2 in the hydrogenation of 4-octyne to *cis*-4-octene in 2-propanol suspensions of Pd(0.2)@Ag(0.5)/TiO_2.

3.3. Catalytic properties of Pd(0.2)@Ag(0.5)/TiO_2 and kinetics in hydrogenation of 4-octyne

Fig. 3 shows time courses of products obtained in photocatalytic reaction of 4-octyne over Pd(0.2)@Ag(0.5)/TiO_2. 4-Octyne was almost quantitatively converted to *cis*-4-octene after 1 h. On the other hand, *trans*-4-octene and octane were not produced before and after 1 h, indicating that isomerization and overhydrogenation of *cis*-4-octene were almost completely suppressed by the introduction of an Ag shell. To evaluate the selectivity of *cis*-4-octene and intermediates in the hydrogenation of 4-octyne and the stoichiometric balance between photocatalytic oxidation and reduction, two indicators, *i.e.*, material balance (MB) and redox balance (RB), were calculated from Eqs. (4) and (5), respectively:

$$\text{MB} = \frac{\text{n(4-Octyne)} + \text{n}(cis/trans\text{-4-Octene}) + \text{n(Octane)}}{\text{n}_0\text{(4-Octyne)}} \quad (4)$$

$$\text{RB} = \frac{\text{n}(cis/trans\text{-4-Octene}) + 2\text{n(Octane)} + \text{n}(\text{H}_2)}{\text{n(Acetone)}} \quad (5)$$

where n(4-Octyne), n(*cis*/*trans*-4-Octene), n(Octane), n(H_2) and n(Acetone) are the amounts of 4-octyne, *cis*/*trans*-4-octene, octane, H_2 and acetone during the photocatalytic reaction, respectively, and n_0(4-Octyne) is the amount of 4-octyne before the photocatalytic reaction. The values of MB and RB were close to 1.0, indicating that formation of stable intermediates was negligible and acetone was the sole product of

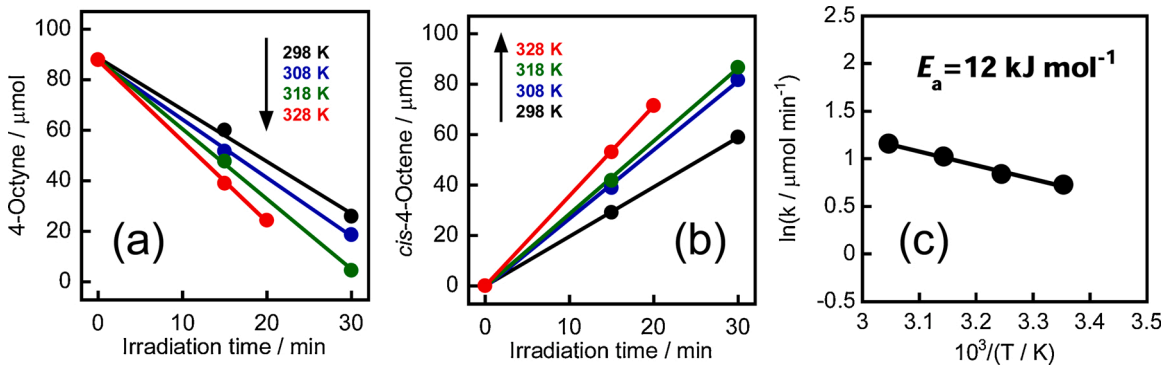

Fig. 5. Time courses of the amounts of (a) 4-octyne remaining and (b) *cis*-4-octene formed in 2-propanol suspensions of a Pd(0.2)@Ag(0.5)/TiO_2 photocatalyst at various temperatures. (c) Arrhenius plot (logarithm of *k vs.* reciprocal of *T*).

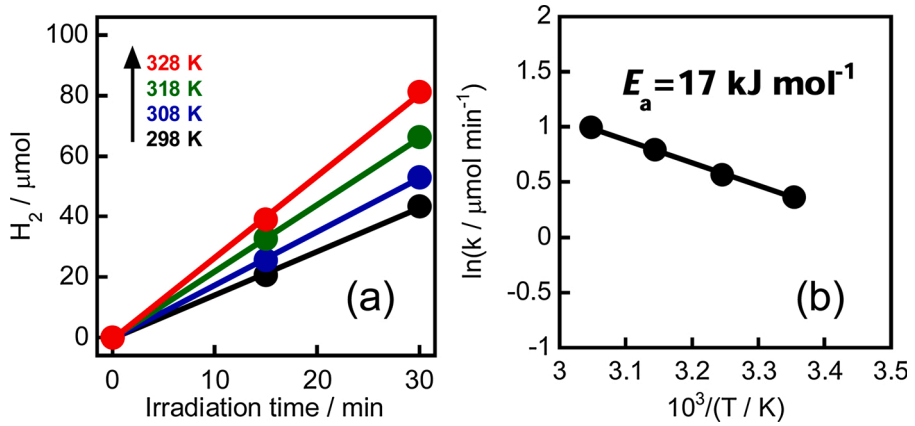

Fig. 6. Time courses of the amounts of (a) H_2 formed from 2-propanol suspensions of a Pd(0.2)@Ag(0.5)/TiO_2 photocatalyst at various temperatures. (b) Arrhenius plot (logarithm of *k vs.* reciprocal of *T*).

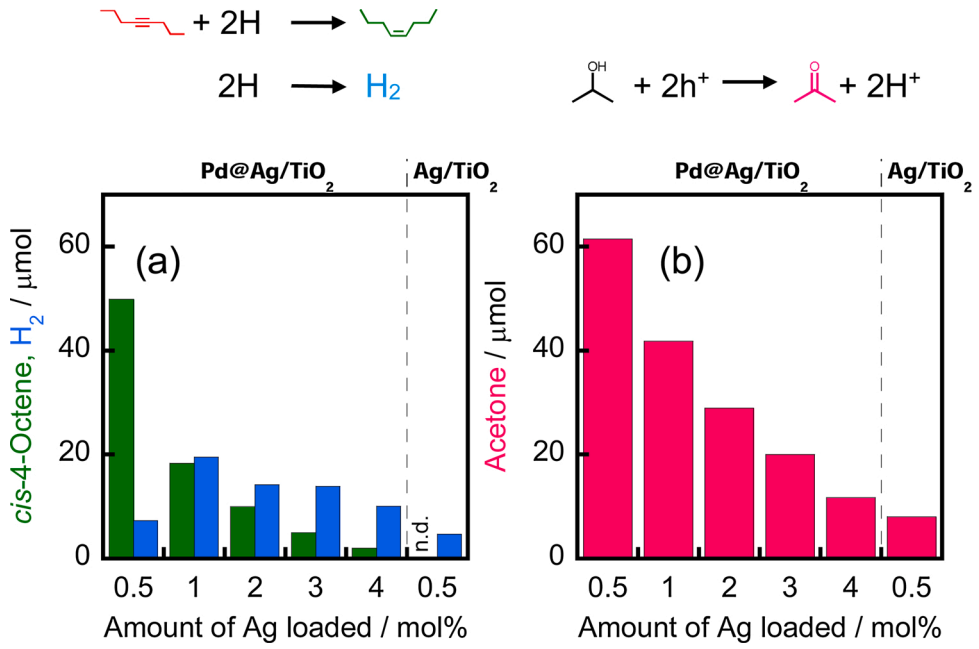

Fig. 7. Amounts of (a) *cis*-4-octene, H_2 and (b) acetone in 2-propanol suspensions of Pd(0.2)@Ag(X)/TiO_2 and Ag(0.5)/TiO_2 under a deaerated condition (irradiation time: 0.5 h).

Table 3
Values of efficiency of active hydrogen species utilization on photocatalytic hydrogenation of 4-octyne over various photocatalysts.

Photocatalyst	EHU[a] / %
$Pd(0.2)@Ag(0.5)/TiO_2$	81
$Pd(0.2)@Ag(1.0)/TiO_2$	44
$Pd(0.2)@Ag(2.0)/TiO_2$	34
$Pd(0.2)@Ag(3.0)/TiO_2$	25
$Pd(0.2)@Ag(4.0)/TiO_2$	17
$Ag(0.5)/TiO_2$	0

[a] EHU was calculated from following equation. $EHU = \frac{n(cis\text{-4-Octene})}{n(Acetone)} \times 100$.

Table 4
Values of activation energy of photocatalytic hydrogenation of 4-octyne and H_2 evolution from 2-propanol over various photocatalysts.

Photocatalyst	E_a / kJ mol^{-1}	
	Hydrogenation of 4-octyne	H_2 evolution
$Pd(0.2)/TiO_2$	11	12
$Pd(0.2)@Ag(0.5)/TiO_2$	12	17
$Pd(0.2)@Ag(2.0)/TiO_2$	17	21
$Pd(0.2)@Ag(3.0)/TiO_2$	20	23
$Pd(0.2)@Ag(4.0)/TiO_2$	45	26
$Ag(0.5)/TiO_2$	–	30

oxidation. The excellence of the $Pd(0.2)@Ag(0.5)/TiO_2$ photocatalyst is that H_2 evolution barely occurs during hydrogenation of 4-octyne. Based on the results of hydrogenation over co-catalyst-loaded TiO_2, this reaction is described as follows: 1) positive holes and electrons are formed under UV light irradiation, 2) 2-propanol is oxidized by positive holes, resulting in the formation of protons and acetone, 3) the protons are reduced by electrons over the Pd@Ag co-catalyst, resulting in the formation of active hydrogen species (AHS), 4) 4-octyne reacts with AHS, producing *cis*-4-octene, and 4') as a side reaction, H_2 is evolved by self-coupling of AHS.

Fig. 4 shows photoabsorption spectra of bare TiO_2 and $Pd(0.2)@Ag(0.5)/TiO_2$. The action spectrum of hydrogenation of 4-octyne to *cis*-4-octene over $Pd(0.2)@Ag(0.5)/TiO_2$ is also shown in Fig. 4, indicating that AQE showed a tendency similar to the absorption spectrum of bare TiO_2. This result means that this reaction was induced by photoabsorption of TiO_2. The value of AQE calculated from Eq. (6) was 29.4 % at 331 nm. In the range of ca. 400–450 nm, Ag nanoparticles often show surface plasmonic resonance (SPR) and may induce photocatalytic reaction. However, the action spectrum means that SPR of Ag nanoparticles in $Pd(0.2)@Ag(0.5)/TiO_2$ does not contribute to the hydrogenation under the present condition.

To understand the high selectivity of hydrogenation over $Pd(0.2)@Ag(0.5)/TiO_2$, reactions were carried out at various temperatures under irradiation of light from a UV-LED. The kinetics was evaluated from the apparent activation energy (E_a) on hydrogenation of 4-octyne and H_2 evolution in a 2-propanol suspension of $Pd(0.2)@Ag(0.5)/$

Table 5
Effects of reaction conditions on hydrogenation of 4-octyne for 1 h at 293 K[a].

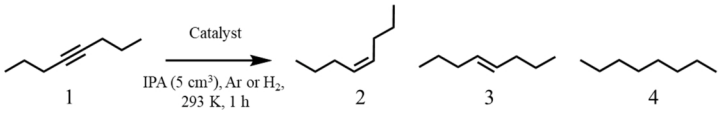

Entry	UV	Catalyst	Gas phase	Conv. of 1[b] / %	Sel. of 2[b] / %	Sel. of 3[b] / %	Sel. of 4[b] / %
1	On	$Pd@Ag/TiO_2$	Ar	>99	99	1	0
2	On	–	Ar	0	0	0	0
3	–	$Pd@Ag/TiO_2$	Ar	0	0	0	0
4	–	Pd/TiO_2	H_2	>99	0	0	93
5	–	Ag/TiO_2	H_2	0	0	0	0
6	–	$Pd@Ag/TiO_2$	H_2	20	>99	0	0

[a] Reaction conditions: $Pd(0.2)@Ag(0.5)/TiO_2$ (50 mg), substrate (*ca.* 60 μmol), 2-propanol (5 cm^3), 293 K and under Ar or H_2.
[b] Determined by GC using an internal standard.

Table 6
Photocatalytic hydrogenation of various alkynes in 2-propanol suspensions of $Pd(0.2)@Ag(0.5)/TiO_2$ at 293 K.[a]

Entry	Substrate	Product	Irradiation time / h	Conv.[b] / %	Sel.[b] / %
1	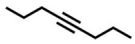	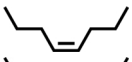	2	>99	>99
2[c]	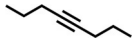		2	>99	>99
3[d]	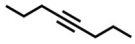		2	>99	>99
4	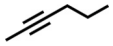	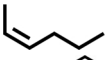	3	>99	93
5	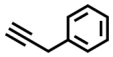	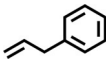	3	>99	94
6	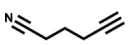	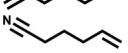	5	>99	94
7	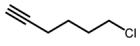	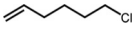	5	>99	80

[a] Reaction conditions: $Pd(0.2)@Ag(0.5)/TiO_2$ (50 mg), substrate (*ca.* 60 μmol), 2-propanol (5 cm^3), 293 K and under Ar.
[b] Determined by GC using an internal standard.
[c] Second use.
[d] Third use.

TiO_2. Fig. 5(a) and (b) show time courses of the amounts of 4-octyne and *cis*-4-octene at various reaction temperatures, respectively. The rates of 4-octyne consumption and *cis*-4-octene production increased with increase in the reaction temperature, and the rate constants were determined on the basis of zero-order kinetics. From the slope of an Arrhenius plot shown in Fig. 5(c), the value of E_a was determined to be 12 kJ mol^{-1}. Compared with values of E_a of the hydrogenation over Cu/TiO_2 (54 kJ mol^{-1}) [20] and $Pd@Cu/TiO_2$ (25 kJ mol^{-1}) [21], the much smaller value of E_a means that a Pd core and an Ag shell are a good combination for selective hydrogenation of 4-octyne.

To obtain information about the side reaction, *i.e.*, H_2 evolution, UV irradiation to 2-propanol suspensions of $Pd(0.2)@Ag(0.5)/TiO_2$ in the *absence* of 4-octyne was carried out at various temperatures, in which only H_2 was produced because there was no other electron acceptor. Fig. 6(a) and (b) show the results and an Arrhenius plot, respectively, and E_a of H_2 evolution was determined to be 17 kJ mol^{-1}. High selectivity of $Pd(0.2)@Ag(0.5)/TiO_2$ for 4-octyne hydrogenation is explained by the value of E_a for 4-octyne hydrogenation being smaller than the value of E_a for H_2 evolution. Production of H_2 means that AHS are not selectively used for hydrogenation. We think that efficiency of AHS utilization (EHU) is important as well as hydrogenation selectivity and will discuss EHU in the next section.

3.4. Effect of Ag content on catalytic properties of $Pd@Ag/TiO_2$

To investigate the catalytic properties of $Pd@Ag/TiO_2$ having various thicknesses of the Ag shell, hydrogenation of 4-octyne over $Pd(0.2)@Ag(X)/TiO_2$ was carried out for 0.5 h and values of EHU on the hydrogenation were compared. Fig. 7(a) and (b) show the amounts of the reduction product (*cis*-4-octene and H_2) and oxidation product (acetone) in 2-propanol suspensions. The amounts of *cis*-4-octene and acetone monotonically decreased when the thickness of the Ag shell increased. On the other hand, the amount of H_2 evolved reached a maximum at X = 1.0 and then decreased with increase in X. 4-Octyne barely hydrogenated to *cis*-4-octene at X = 4.0, indicating that most of the AHS were used for H_2 evolution. In addition, only H_2 evolution occurred over Pd-free $Ag(0.5)/TiO_2$. From these results, values of EHU for the hydrogenation were calculated and are summarized in Table 3, indicating that the maximum value of EHU (81 %) was obtained at X = 0.5. EHU was calculated from Eq. (6):

$$\mathrm{EHU} = \frac{\mathrm{n}(\textit{cis}\text{-4-Octene})}{\mathrm{n}(\mathrm{Acetone})} \times 100 \quad (6)$$

Values of E_a for hydrogenation and H_2 evolution over Pd-free $Ag(0.5)/TiO_2$ and $Pd(0.2)@Ag(X)/TiO_2$ are shown in Table 4. The values of E_a for hydrogenation gradually increased when the thickness of the Ag shell increased and drastically increased at X = 4.0. Since no hydrogenation occurred even at 328 K, E_a of Pd-free $Ag(0.5)/TiO_2$ was not determined, suggesting that the value of E_a is very large. The change in E_a for H_2 evolution was small compared with the change in the E_a for hydrogenation, and the catalytic properties of $Pd(0.2)@Ag(X)/TiO_2$ became close to those of $Ag(0.5)/TiO_2$ as shown in Table 4. Interestingly, the value of E_a for hydrogenation became larger than that of E_a for H_2 evolution at X = 4.0.

3.5. Effects of reaction conditions

Table 5 shows the effects of photoirradiation, co-catalyst and atmosphere of gas phase on hydrogenation of 4-octyne at 293 K. Photoirradiation to 4-octyne in the presence of $Pd(0.2)@Ag(X)/TiO_2$ under Ar for 1 h produced *cis*-4-octene almost quantitatively (Entry 1). No hydrogenation occurred under $Pd(0.2)@Ag(X)/TiO_2$-free and light-free conditions (Entries 2 and 3). Entries 4-6 show the results of thermal reactions at 293 K under H_2 (1 atm) for 1 h. In the presence of $Pd(0.2)/TiO_2$, 4-octyne was deeply hydrogenated to octane (Entry 4). No hydrogenation of 4-octyne occurred over $Ag(0.5)/TiO_2$ even under H_2 (Entry 5). Thermal catalysis of Pd nanoparticles was controlled by introducing an Ag shell and *cis*-4-octene was produced selectively (Entry 6). However, the rate of the thermal reaction was about one-fifth of that of the photocatalytic reaction (Fig. 3), suggesting that formation of AHS by photocatalytic reduction of H^+ on Pd@Ag nanoparticles occurs more easily than that by dissociative adsorption of molecular H_2.

Effect of the light intensity on the *cis*-4-octene yield was examined (Fig. S3). Larger yield of *cis*-4-octene was obtained under more intense light; however, the yield gradually saturated just like a logarithmic curve. In other words, a modest yield can be obtained under light intensity of several mW cm^{-2}, which is almost equal to that of solar light.

3.6. Reusability and applicability of $Pd@Ag/TiO_2$

Table 6 shows the results of re-use of $Pd@Ag/TiO_2$ for hydrogenation of 4-octyne and use of $Pd@Ag/TiO_2$ for hydrogenation of other alkynes. After the first use (Entry 1), $Pd@Ag/TiO_2$ still showed high performance for 4-octyne hydrogenation in the second and third uses (Entries 2 and 3). *cis*-Selectivity was also achieved in hydrogenation of 2-hexyne (Entry 4). $Pd@Ag/TiO_2$ also worked in hydrogenation of terminal alkynes to corresponding alkenes (Entries 5-7). We noted that $Pd@Ag/TiO_2$ was not active for a carbon-nitrogen triple bond (C≡N) (Entries 6). Interestingly, a chloro group, which is typically a good leaving group, was preserved in hydrogenation of alkyne (Entries 7). Since Pd is very active for elimination of a chloro group from a hydrocarbon [10], this result indicates that the Pd core was almost completely covered with the Ag shell. These results show a wide applicability of the $Pd@Ag/TiO_2$ photocatalyst in hydrogenation of alkynes to alkenes.

4. Conclusion

$Pd@Ag/TiO_2$ having various Ag contents was prepared by using a two-step photodeposition method and used for photocatalytic hydrogenation of alkyne in an alcohol suspension without the use of H_2 gas. Almost quantitative conversion of 4-octyne to *cis*-4-octene was achieved over $Pd(0.2)@Ag(0.5)/TiO_2$, while evolution of H_2 as the by-product barely occurred during the hydrogenation, resulting in high efficiency of AHS in photocatalytic hydrogenation. Reactions at various temperatures revealed that the activation energies for the photocatalytic hydrogenation and H_2 evolution over $Pd(0.2)@Ag(0.5)/TiO_2$ were 12 kJ mol^{-1} and 17 kJ mol^{-1}, respectively, which explains the high value of EHU in the hydrogenation. With increase in the Ag content, the value of E_a in the hydrogenation became close to that in H_2 evolution, resulting in a decrease in the value of EHU in the hydrogenation. An applicability test showed that the $Pd@Ag/TiO_2$ photocatalyst can be used for hydrogenation of various alkynes to alkenes.

Declaration of Competing Interest

The authors declare that they have no known competing financial interests or personal relationships that could have appeared to influence the work reported in this paper.

CRediT authorship contribution statement

Shota Imai: Conceptualization, Investigation, Writing - original draft. **Yasumi Kojima:** Conceptualization, Investigation. **Eri Fudo:** Investigation. **Atsuhiro Tanaka:** Validation, Writing - review & editing. **Hiroshi Kominami:** Supervision, Validation, Writing - review & editing.

Acknowledgements

This work was partly supported by JSPS KAKENHI Grant Numbers 20H02527. A.T. is grateful for financial support from the Faculty of Science and Engineering, Kindai University.

Appendix A. Supplementary data

Supplementary material related to this article can be found, in the online version, at doi:https://doi.org/10.1016/j.apcata.2021.118331.

References

[1] K. Maeda, A. Xiong, T. Yoshinaga, T. Ikeda, N. Sakamoto, T. Hisatomi, M. Takashima, D. Lu, M. Kanehara, T. Setoyama, T. Teranishi, K. Domen, Angew. Chem. Int. Ed. 49 (2010) 4096–4099, https://doi.org/10.1002/anie.201001259.

[2] J. Yang, D. Wang, H. Han, Can Li, Acc. Chem. Res. 46 (2013) 1900–1909, https://doi.org/10.1021/ar300227e.

[3] J. Ran, J. Zhang, J. Yu, M. Jaroniec, S.-Z. Qiao, Chem. Soc. Rev. 43 (2014) 7787–7812, https://doi.org/10.1039/C3CS60425J.

[4] S.-i. Nishimoto, B. Ohtani, T. Kagiya, J. Chem. Soc., Faraday Trans. 1 (81) (1985) 2467–2474, https://doi.org/10.1039/F19858102467.

[5] B. Ohtani, K. Iwai, S.-i. Nishimoto, S. Sato, J. Phys. Chem. B 101 (1997) 3349–3359, https://doi.org/10.1021/jp962060q.

[6] S.E. Salas, B.S. Rosales, H. de Lasa, Appl. Catal. B: Environ. 140-141 (2013) 523–536, https://doi.org/10.1016/j.apcatb.2013.04.016.

[7] J. Zhang, Z. Yu, Z. Gao, H. Ge, S. Zhao, C. Chen, S. Chen, X. Tong, M. Wang, Z. Zheng, Y. Qin, Angew. Chem. Int. Ed. 56 (2017) 816–820, https://doi.org/10.1002/anie.201611137.

[8] G.M. Haselmann, D. Eder, ACS Catal. 7 (2017) 4668–4675, https://doi.org/10.1021/acscatal.7b00845.

[9] D. Wang, Z.-P. Liu, W.-M. Yang, ACS Catal. 8 (2018) 7270–7278, https://doi.org/10.1021/acscatal.8b01886.

[10] K. Fuku, K. Hashimoto, H. Kominami, Chem. Commun. 46 (2010) 5118–5120, https://doi.org/10.1039/C0CC00589D;
K. Fuku, K. Hashimoto, H. Kominami, Catal. Sci. Technol. 1 (2011) 586–592, https://doi.org/10.1039/C0CY00040J.

[11] K. Imamura, Y. Okubo, T. Ito, A. Tanaka, K. Hashimoto, K. Kominami, RSC Adv. 4 (2014) 19883–19886, https://doi.org/10.1039/C4RA02275K.

[12] H. Kominami, S. Yamamoto, K. Imamura, A. Tanaka, K. Hashimoto, Chem. Commun. 50 (2014) 4558–4560, https://doi.org/10.1039/C3CC49340G.

[13] H. Kominami, M. Higa, T. Nojima, T. Ito, K. Nakanishi, K. Hashimoto, K. Imamura, ChemCatChem 8 (2016) 2019–2022, https://doi.org/10.1002/cctc.201600290.

[14] K. Nakanishi, R. Yagi, K. Imamura, A. Tanaka, K. Hashimoto, H. Kominami, Catal. Sci. Technol. 8 (2018) 139–146, https://doi.org/10.1039/C7CY01929G.

[15] T. Mitsudome, T. Urayama, K. Yamazaki, Y. Maehara, J. Yamasaki, K. Gohara, Z. Maeno, T. Mizugaki, K. Jitsukawa, K. Kaneda, ACS Catal. 6 (2016) 666–670, https://doi.org/10.1021/acscatal.5b02518.

[16] T. Mitsudome, Y. Takahashi, S. Ichikawa, T. Mizugaki, K. Jitsukawa, K. Kaneda, Angew. Chem. Int. Ed. 52 (2013) 1481–1485, https://doi.org/10.1002/anie.201207845.

[17] M.K. Kumar, J.Y. Do, A.K. Reddy, M. Kang, Appl. Catal. B: Environ. 231 (2018) 137–150, https://doi.org/10.1016/j.apcatb.2018.03.015.

[18] P. Reyes, G. Pecchi, J.L.G. Fierro, Langmuir 17 (2001) 522–527, https://doi.org/10.1021/la0006418.

[19] K. Kusada, H. Kobayashi, R. Ikeda, Y. Kubota, M. Takata, S. Toh, T. Yamamoto, S. Matsumura, N. Sumi, K. Sato, K. Nagaoka, H. Kitagawa, J. Am. Chem. Soc. 136 (2014) 1864–1871, https://doi.org/10.1021/ja409464g.

[20] H. Kominami, M. Shiba, A. Hashimoto, S. imai, K. Nakanishi, A. Tanaka, K. Hashimoto, K. Imamura, Phys. Chem. Chem. Phys. 20 (2018) 19321–19325, https://doi.org/10.1039/C8CP02316F.

[21] S. Imai, K. Nakanishi, A. Tanaka, H. Kominami, ChemCatChem 12 (2020) 1609–1616, https://doi.org/10.1002/cctc.201902175.

[22] A. Tanaka, K. Hashimoto, H. Kominami, ChemCatChem 3 (2011) 1619–1623, https://doi.org/10.1002/cctc.201100158.

[23] A. Tanaka, K. Hashimoto, H. Kominami, Chem. Eur. J. 22 (2016) 4592–4599, https://doi.org/10.1002/chem.201504606.

[24] R.G. Bai, K. Muthoosamy, F.N. Shipton, A. Pandikumar, P. Rameshkumar, N. M. Huang, S. Manickam, RSC Adv. 6 (2016) 36576–36587, https://doi.org/10.1039/C6RA02928K.

[25] S.H.Y. Lo, Y.-Y. Wang, C.-C. Wan, J. Colloid Interface Sci. 310 (2007) 190–195, https://doi.org/10.1016/j.jcis.2007.01.057.